

# Dynamic Stability Analysis of an Adjustable-Height Single-Arm Mobile Manipulator

Tianqun Yuan<sup>1, 2, 3, 4</sup>, Xiumin Shi<sup>1, 2, 3, 4, \*</sup>, Yuming Qi<sup>1, 2, 3, 4</sup>

<sup>1</sup> School of Mechanical Engineering, Tianjin University of Technology and Education, Tianjin 300350, China

<sup>2</sup> Institute of Robotics and Intelligent Equipment, Tianjin University of Technology and Education, Tianjin, China

<sup>3</sup> Tianjin Key Laboratory of Intelligent Robot Technology and Application, Tianjin, China

<sup>4</sup> Tianjin Bonus Robotics Technology Co., Ltd, Tianjin, China

\* Corresponding Author: Xiumin Shi (Email: [sxmzzy123@163.com](mailto:sxmzzy123@163.com))

---

## ABSTRACT

This study investigates the overturning stability of a self-developed, adjustable-height single-arm mobile manipulator during operations involving height variations and load-bearing tasks. Static and dynamic stability analyses were conducted to evaluate system performance. Under no-load and low-speed conditions, static stability was assessed using the gravity method. For typical operational scenarios with variable loads and changing arm heights, a dynamic stability criterion based on the Tip-Over Moment (TOM) was proposed, accompanied by the establishment of a system dynamics model and a comprehensive evaluation framework incorporating mean value and standard deviation metrics. Through co-simulations in MATLAB and ADAMS, the dynamic performance was examined under various combinations of load mass and manipulator height. Results indicate that the system maintains stability across all tested conditions. Increasing the load mass was found to enhance system stability, while elevating the arm height, despite improving the overall anti-overturning tendency, was observed to amplify moment fluctuations. This research provides a theoretical foundation for structural optimization and stable motion control of this class of adjustable-height single-arm mobile manipulators.

## KEYWORDS

Adjustable-height Single-arm Mobile Manipulator; Anti-overturning Stability; Tip-Over Moment.

---

## 1. INTRODUCTION

Conventional robotic arms are typically mounted on a stationary base, which constrains their workspace and often leads to unreachable end-effector targets [1]. To overcome this limitation and expand the operational workspace, the manipulation capability of the robotic arm has been integrated with the mobility of a platform, resulting in the development of the adjustable-height single-arm mobile manipulator[2]. This type of robot effectively mitigates the drawbacks of fixed-base arms, such as limited workspace and poor flexibility, by introducing additional degrees of freedom and enhancing overall manipulation performance. Consequently, it has attracted significant research interest [3]. However, the unique structure of the adjustable-height single-arm mobile manipulator means that the arm can generate substantial overturning moments on the mobile platform during operation, potentially leading to tip-over. Such incidents can cause damage to platform components, loss of control, and operational failure [4].

Furthermore, specific arm motions can exacerbate this tipping risk, necessitating a thorough investigation into the dynamic effects of arm movement on platform stability [5,6] to ensure reliable operation. Song Tao from Shanghai University [7] analyzed the tip-over tendency of conventional mobile manipulators using a Tip-over Moment (TOM) criterion based on the moment generated about the potential tipping axis. Zhou Likun et al. [8] applied the dynamic energy stability cone method to analyze the stability of a tank-cleaning robot during operation, validating their structural design through ADAMS simulations. Yun Jintian et al. [9] addressed the tipping and sliding risks when a nursing robot lifts a patient, using the Center of Gravity Projection method and the Zero-Moment Point criterion to evaluate stability in static and dynamic phases, respectively. Zang Jiannan [10] systematically developed a stability model for extreme postures based on the stability cone method and proposed critical tip-over conditions.

The adjustable-height single-arm mobile manipulator offers distinct advantages in warehouse logistics and material handling due to its mobility and adaptability. Nonetheless, ensuring its anti-tip stability during task execution is paramount for safe deployment. Therefore, this paper presents a comprehensive stability analysis by integrating the Gravity Projection method and a time-varying TOM method. Both static and dynamic stability are systematically evaluated, and the effectiveness of the approach, along with system performance, is verified through co-simulations using MATLAB and ADAMS.

## 2. MATHEMATICAL MODELING OF THE MANIPULATOR

### 2.1. Kinematic Modeling of the Manipulator

The overall system comprises a wheeled mobile platform, a lifting mechanism, a robotic arm, and the associated control hardware. A model of the adjustable-height single-arm mobile manipulator is presented in Fig. 1.



**Figure 1.** Model of the Adjustable-Height Single-Arm Mobile Manipulator

This study conducts the kinematic modeling of a self-developed, lightweight, and compliant robotic arm designed for human-robot collaboration, which features a high payload-to-weight ratio. The lifting mechanism is integrated as a prismatic joint within the arm's kinematic chain. Using the Modified Denavit-Hartenberg (MDH) method, link coordinate frames are established at each joint, including the lifting joint, to derive a complete kinematic model of the adjustable-height single-arm mobile manipulator, as illustrated in Fig .2.

Based on the established model and joint parameters, the corresponding kinematic parameters for the adjustable-height single-arm mobile manipulator are derived and presented in Table 1.

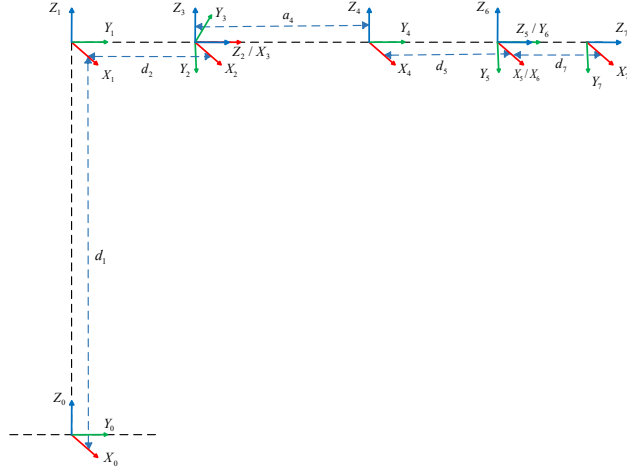


**Figure 2.** Schematic of the Manipulator Joint Coordinates

**Table 1.** Kinematic Parameters of the Manipulator

$i$	$a_{i-1}/\text{mm}$	$\alpha_{i-1}/[^\circ]$	$d_i/\text{mm}$	$\theta_i/\text{offset}_i[^\circ]$
1	0	0	0-1000	0
2	0	-90	240.5	0
3	0	90	0	90
4	256	0	0	0
5	0	-90	210	0
6	0	90	0	0
7	0	-90	144	0

The MDH parameters for the established link coordinate frames are:  $a_{i-1}$ : Link length – offset along  $X_{i-1}$  from  $Z_{i-1}$  to  $Z_i$ ;  $\alpha_{i-1}$ : Link twist – rotation about  $X_{i-1}$  from  $Z_{i-1}$  to  $Z_i$ ;  $d_i$ : Link offset – offset along  $Z_i$  from  $X_{i-1}$  to  $X_i$ ;  $\theta_i$ : Joint angle – rotation about  $Z_i$  from  $X_{i-1}$  to  $X_i$ ; offset: Zero-position deviation between mechanical and modeling reference.

## 2.2. Dynamic Modeling of the Manipulator

The critical need for real-time tip-over stability evaluation in the adjustable-height single-arm mobile manipulator necessitates a computationally efficient dynamic model. Consequently, the recursive Newton-Euler method was employed to derive the system's dynamic equations. The implementation of this method first requires acquiring the inertial parameters of the manipulator links—namely, their masses, center-of-mass positions, and inertia tensors. These parameters were efficiently acquired by defining the materials and coordinate systems in SolidWorks and subsequently exporting the complete inertial dataset.

The forward recursion of the Newton-Euler method entails an outward computation of link velocities and accelerations, starting from link 1. The equations are given below:

Forward Recursion for Angular Velocity:

$$\begin{cases} {}^i\omega_{i+1} = {}^i\omega_i + {}^{i+1}R^i q_{i+1} \square {}^{i+1}Z_{i+1} \\ {}^{i+1}\omega_{i+1} = {}^{i+1}R^i {}^i\omega_i + q_{i+1} \square {}^{i+1}Z_{i+1} \end{cases}, \quad (1)$$

Forward Recursion for Angular acceleration:

$${}^{i+1}\omega_{i+1} \square = {}^{i+1}R^i \omega_i \square + q_{i+1} \square {}^{i+1}Z_{i+1} + {}^{i+1}R^i \omega_i \times q_{i+1} \square {}^{i+1}Z_{i+1}, \quad (2)$$

Forward Recursion for Linear Velocity :

$${}^{i+1}v_{i+1} = {}^{i+1}R^i \left[ {}^i v_i + \omega_i \times {}^i O_{i+1} + {}^i \omega_i \times ({}^i \omega_i \times {}^i O_{i+1}) \right], \quad (3)$$

In the equation:  $\omega_i$  denotes the angular velocity of link  $i$ ;  ${}^i \omega_i$  and  ${}^{i+1} \omega_{i+1}$  represent the angular velocities of link  $i$  and link  $i+1$ , expressed in their own coordinate systems, respectively;  ${}^{i+1}R^i$  is the rotation matrix transforming the coordinate system from link  $i$  to link  $i+1$ ;  $q_{i+1}$  refers to the angular velocity of joint  $i+1$ ;  $Z_{i+1}$  denotes the unit vector along the Z-axis of the coordinate system attached to link  $i+1$ ;  ${}^i v_i$  and  ${}^{i+1} v_{i+1}$  represent the linear velocities of the origin of the coordinate system on link  $i$  and link  $i+1$ , respectively;  ${}^i P_{i+1}$  is the position vector from the origin of the coordinate system on link  $i$  to that on link  $i+1$ , expressed in the coordinate system of link  $i$ .

The interaction forces and moments between adjacent links are computed recursively from link  $n$  to link 1 (backward recursion), as follows:

$$\left\{ \begin{array}{l} {}^{i+1}F_{i+1} = m_{i+1} v_{Ci+1} \\ {}^{i+1}N_{i+1} = C_{i+1} I_{i+1} \omega_{i+1} + {}^{i+1} \omega_{i+1} \times C_{i+1} I_{i+1} {}^{i+1} \omega_{i+1} \end{array} \right., \quad (4)$$

The manipulator constitutes a multibody dynamic system where each link is acted upon not only by inertial forces and moments at its center of mass but also by constraint wrenches from adjacent links. The net force and moment on each link are derived by superimposing all these components. This superposition leads to the equilibrium equations, which, when rearranged, yield:

$$\left\{ \begin{array}{l} {}^i f_i = {}^i F_i + {}^{i+1}R^i {}^{i+1} f_{i+1} \\ {}^i n_i = {}^i N_i + {}^{i+1}R^i {}^{i+1} n_{i+1} + {}^i O_{ci} \times {}^i F_i + {}^i O_{i+1} \times {}^{i+1}R^i {}^{i+1} f_{i+1} \end{array} \right., \quad (5)$$

In the equation:  ${}^i f_i$  and  ${}^{i+1} f_{i+1}$  denote the forces acting on link  $i$  and link  $i+1$ , respectively;  ${}^i n_i$  and  ${}^{i+1} n_{i+1}$  denote the moments acting on link  $i$  and link  $i+1$ , respectively.

### 3. STABILITY ANALYSIS UNDER NO-LOAD OPERATION

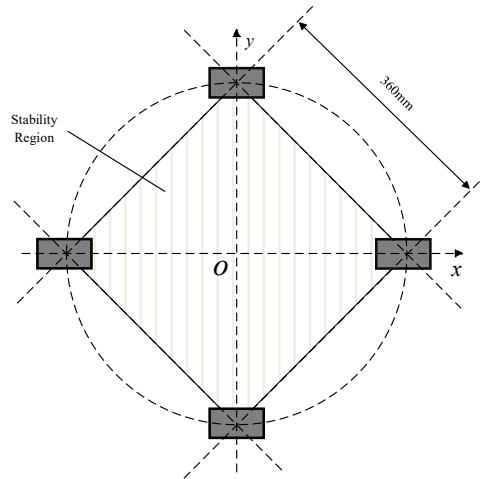


Figure 3. Stability Region

Under no-load and low-speed operating conditions, the dynamic stability of the adjustable-height single-arm mobile manipulator can be evaluated via a quasi-static assumption, postulated as a sequence of continuous static equilibrium states. Under this assumption, system stability is determined using the gravity projection method. A convex polygon, termed the stability region, is defined in the horizontal plane by the contact points between the robot's driving wheels and the ground. As illustrated in Fig. 3, to ensure the robot is free from overturning, the horizontal projection of the system's center of mass must perpetually lie within the boundaries of this stability region.

The stability condition for the adjustable-height single-arm mobile manipulator requires that the maximum lateral and longitudinal center-of-mass offsets must fulfill:  $x_{\max}, y_{\max} \leq 360\text{mm}$ .

The components of the robot's center of mass are:

$$\left. \begin{aligned} x_c &= \frac{\sum_{i=1}^n x_i \cdot m_i}{M} \\ y_c &= \frac{\sum_{i=1}^n y_i \cdot m_i}{M} \\ z_c &= \frac{\sum_{i=1}^n z_i \cdot m_i}{M} \end{aligned} \right\}, \quad (6)$$

Where  $m_i$  is the mass of link  $i$ ;  $(x_i, y_i, z_i)$  is the position coordinate of the center of mass of link  $i$  in the absolute coordinate system  $O_{x_0, y_0, z_0}$ , and  $M$  is the total mass of the Adjustable-Height Single-Arm Mobile Manipulator.

The three-dimensional model of the designed adjustable-height single-arm mobile manipulator was imported into the ADAMS virtual simulation environment. The simulation was configured with the following conditions: the robot was to perform uniform linear motion on a smooth surface, with no load applied at the end-effector and with both the lifting mechanism and the robotic arm maintaining a fixed pose throughout the motion. The material properties were defined as rigid bodies, and the corresponding kinematic constraints were applied without applying external forces to the end-effector. The total simulation time was set to 15 seconds with an integration step size of 0.05 seconds. The trajectories of the center of mass for each component along the X, Y, and Z axes are presented in Fig. 4(a) to 4(c). The overall trajectory of the system's center of mass in space during the entire motion, obtained by substituting the component centroid data into Eq. 6, is shown in Fig.5.

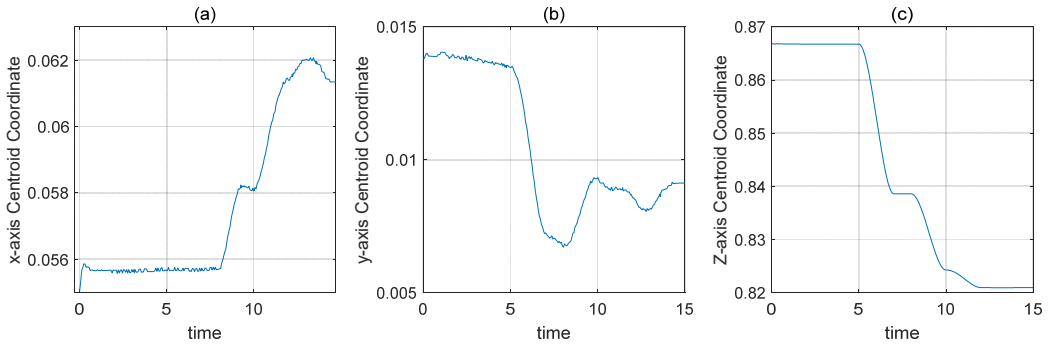


**Figure 4.** Center-of-Mass Displacements along Principal Axes

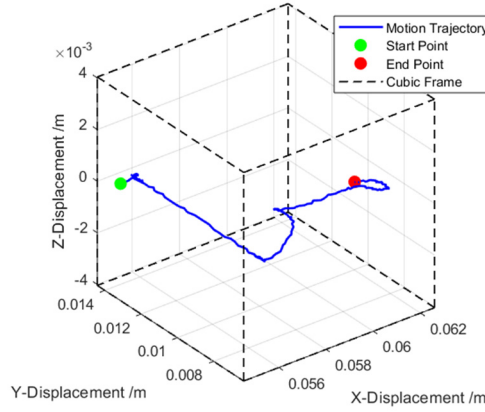


**Figure 5.** System Center-of-Mass Trajectory

As evidenced by Fig. 4 and Fig. 5, the maximum recorded displacement of the system's center of mass was 7 mm in the X-direction and 4 mm in the Y-direction. Given that these displacements are well within the boundaries of the predefined stability region, it is conclusively demonstrated that the adjustable-height single-arm mobile manipulator maintained a stable state without any tendency to overturn during its no-load, low-speed operational profile.

## 4. DYNAMIC STABILITY ANALYSIS OF AN ADJUSTABLE-HEIGHT SINGLE-ARM MOBILE MANIPULATOR

### 4.1. Criteria for Stability Assessment

The dynamic model of the adjustable-height single-arm mobile manipulator is based on the following simplifying assumptions: the ground is idealized as a perfectly planar and rigid surface, with all inclination, irregularities, and deformations neglected; all wheels maintain continuous point contact with the ground, and wheel slip is excluded from consideration; furthermore, the entire system—including the mobile platform, lifting mechanism, manipulator links, and joints—is treated as an assembly of rigid bodies, with structural flexibilities and wheel deformations not considered.

Fig.6 shows the free-body diagram of the adjustable-height single-arm mobile manipulator, with the ellipse representing the mobile platform. Key loads include: the lifting mechanism's action on Joint 1  $1[f_M \quad N_M]^T$ , the end-effector payload gravity  $f_A$ , the system's gravitational force  $f_g$ , and the inertial force  $f_I$ . The corresponding reaction wrench from the manipulator arm on Joint 1 is  $-\omega_1$ :

$$-\omega_1 = [f_M^T, n_M^T]^T. \quad (7)$$

Where  $f_M$  and  $n_M$  consist of components along the X, Y, and Z axes:

$$f_M = [f_X, f_Y, f_Z]^T. \quad (8)$$

$$n_M = [n_X, n_Y, n_Z]^T. \quad (9)$$

The wheel-ground interactions are modeled as point contacts. The set of these contact points for the six-wheeled platform defines a hexagon in the horizontal plane. Each side of this hexagon corresponds to a potential tip-over axis. The model stipulates that the adjustable-height single-arm mobile manipulator can only overturn by pivoting around one of these predefined axes. The

coordinates of two adjacent vertices defining the hexagonal support polygon are denoted as  $P_i$  and  $P_{i+1}$ . The unit vector  $a_{ii+1}$  along the tip-over axis connecting these points is given by:

$$a_{ii+1} = \frac{P_{i+1} - P_i}{|P_{i+1} - P_i|}, \quad (10)$$

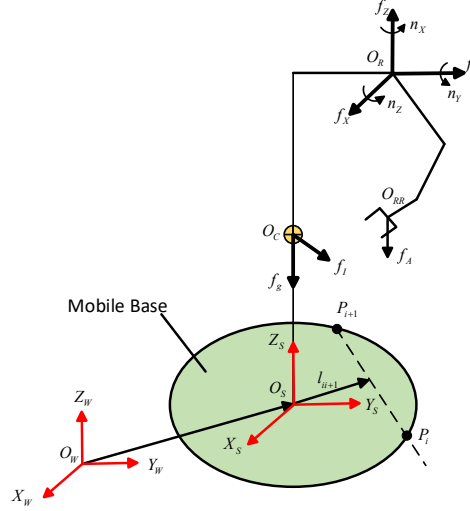


**Figure 6.** Force Analysis of the Adjustable-Height Single-Arm Mobile Manipulator

The TOM of the system about the overturning axis is:

$$\text{TOM} = \left[ (f_g \times l_{ii+1}) + f_I \times l_{ii+1} \right] \square a_{ii+1} + m_M \square a_{ii+1} + (f_M \times d_{ii+1}) \square a_{ii+1} + (f_A \times s_{ii+1}) \square a_{ii+1}, \quad (11)$$

In eq.11, the first term corresponds to the resultant moment arising from gravitational and inertial effects of the lifting mechanism and mobile platform; the second term represents the constraint moment at Joint 1 of the manipulator; the third term denotes the constraint force at the same joint; and the fourth term quantifies the moment exerted by the end-effector load about the tip-over axis. Here,  $l_{ii+1}$ ,  $d_{ii+1}$ , and  $s_{ii+1}$  denote the perpendicular vectors from points  $O_s$ ,  $O_R$ , and  $O_{RR}$ , respectively, to the tip-over axis  $a_{ii+1}$ .

For the adjustable-height single-arm mobile manipulator, the maximum tip-over moment acting on each potential tip-over axis of the mobile platform is determined by evaluating all corresponding moment values. This maximum is defined as:

$$T_{\max} = \max \{ TOM_1, TOM_2, \dots, TOM_n \}, \quad (12)$$

Given that the system possesses six tip-over axes, six distinct tip-over moment values are computed. The overall maximum  $T_{\max}$  is identified by comparing the magnitudes of these six values. System stability is then assessed as follows: if  $T_{\max} > 0$ , the system will tip over about the axis corresponding to  $T_{\max}$ ; if  $T_{\max} \leq 0$ , the system remains stable.

## 4.2. Stability Analysis Under Loaded Conditions

During handling operations, the payload at the end-effector of the adjustable-height single-arm mobile manipulator induces dynamic coupling between the manipulator's motion and that of the mobile platform, consequently influencing the overall system stability. To analyze the effect of this coupling on the platform's state, the following simulation scenario was configured: the adjustable-

height single-arm mobile manipulator grasps objects with masses of 1 kg, 3 kg, and 5 kg, respectively, and then executes a uniform linear motion while maintaining a constant arm height. This investigation focuses on the influence of different payloads on the tip-over moment generated about the robot's tip-over axes. The simulation was run for a duration of 20 seconds with an integration time step of 0.02 seconds. By substituting the acquired data for joint positions, velocities, and accelerations into Eq.11, the maximum tip-over moment,  $T_{\max}$ , during the motion was computed. The resulting variation curves of  $T_{\max}$  for each payload, under three distinct manipulator heights, are presented in Fig. 7(a) to 7(c).

For the stability assessment, the mean (Mean) and standard deviation (Std) were adopted as evaluation metrics. The justification for this selection is twofold: the Mean reflects the average magnitude of the tip-over moment over the time history, thereby delineating the system's overall tendency to tip over; the Std quantifies the magnitude of moment fluctuations, serving as an indicator of the system's dynamic smoothness during motion. Together, these metrics provide a dual-aspect evaluation of the system's dynamic stability—encompassing both the average level and fluctuation characteristics—and thus establish a quantitative basis for analyzing the influence of both payload and manipulator height on tip-over behavior. The corresponding values of each metric, obtained from the simulation data, are summarized in Table 2.

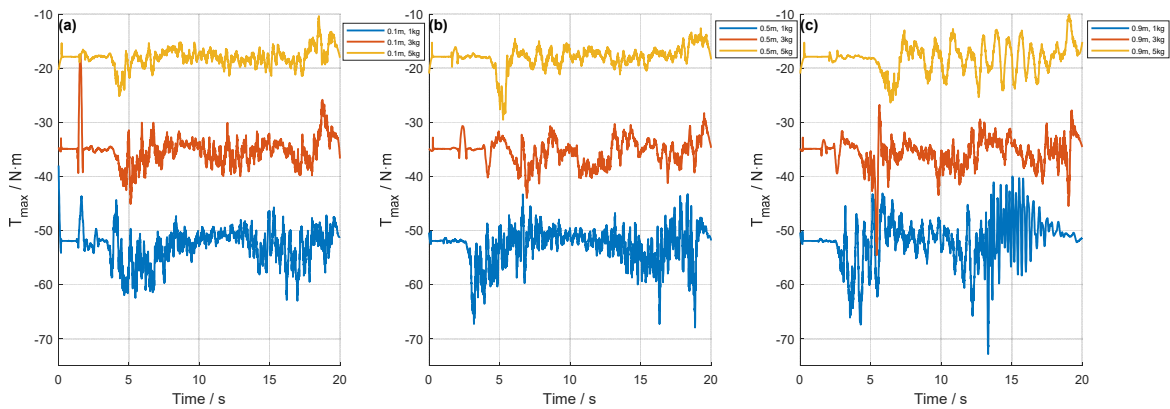


**Figure 7.**  $T_{\max}$  Variation under Varying Payload Conditions

**Table 2.** Stability Indices Across Manipulator Heights and Payload Masses (Mean±Std)

		Manipulator Height [m]		
		1	3	5
Payload Mass [kg]	0.1	-52.76(3.1032)	-35.197(2.744)	-17.982(1.672)
	0.5	-52.867(3.288)	-35.365(2.287)	-17.918(1.974)
	0.9	-51.874(4.327)	-35.617(2.727)	-18.15(2.598)

Based on the data presented in Fig.7 and Table 2, the tip-over moment analysis confirms that the maximum tip-over moment of the adjustable-height single-arm mobile manipulator remains negative under the specified operating condition, indicating sustained stability throughout the motion. At a fixed manipulator height, the system's maximum tip-over moment exhibits a consistent trend as the payload increases from 1 kg to 5 kg. For instance, at the 0.1 m height, the absolute value of the Mean decreases from -52.76 N·m to -17.982 N·m, suggesting that the overall moment level approaches zero and the system's tendency to tip over is consequently reduced. Concurrently, the Std drops from 3.1032 to 1.6718, indicating a significant reduction in moment fluctuations and improved dynamic smoothness. These observed trends demonstrate that an increase in payload effectively diminishes the tip-over risk and enhances the dynamic performance of the adjustable-height single-arm mobile

manipulator in terms of both average level and dynamic smoothness. This finding provides a critical foundation for formulating subsequent strategies for tip-over prevention and control.

### 4.3. Stability Analysis Under Varying Manipulator Height

During handling operations, the vertical movement of the manipulator in the adjustable-height single-arm mobile manipulator modifies the system's overall center-of-mass distribution and inertial properties, thereby intensifying the dynamic coupling between the manipulator and the mobile platform and influencing operational stability. To examine the effect of manipulator height variation on system stability, the following comparative simulation scenarios were designed: the adjustable-height single-arm mobile manipulator grasps objects of fixed mass (1 kg, 3 kg, and 5 kg, respectively) and, under constant load, adjusts the manipulator to different heights (0.1 m, 0.5 m, 0.9 m) via the lifting mechanism, performing uniform linear motion at each height. The analysis focuses on the influence of manipulator height on the tip-over moment about the system's tip-over axes. The variation curves of the maximum tip-over moment,  $T_{\max}$ , for each manipulator height under the three different load conditions are shown in Fig.8(a) to 8(c).

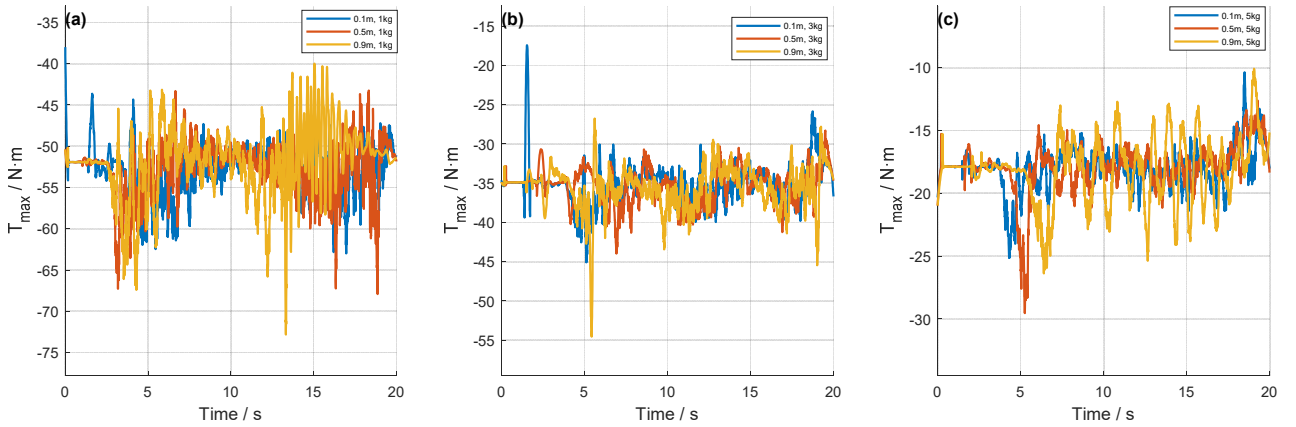


**Figure 8.**  $T_{\max}$  Variation under Varying Manipulator Height Conditions

Based on the data presented in Fig. 8 and Table 2, the maximum tip-over moment of the adjustable-height single-arm mobile manipulator remains negative under the specified conditions, confirming system stability throughout the motion. Under constant load, the maximum tip-over moment exhibits a consistent trend as the manipulator height increases from 0.1 m to 0.9 m. With a 1 kg load, the Mean changes from  $-52.76 \text{ N}\cdot\text{m}$  to  $-51.87 \text{ N}\cdot\text{m}$ , converging toward zero and indicating a reduced overall tipping tendency. However, the Std increases from 3.10 to 4.33, signifying amplified moment fluctuations and diminished motion smoothness. This pattern persists under 3 kg and 5 kg loads, consistently demonstrating Means approaching zero along with elevated Std values.

These trends reveal the dual effect of manipulator height variation on system stability: while increased height attenuates the overall tipping tendency, it amplifies moment fluctuations, thereby introducing greater instability risks. This behavior originates from the reconfiguration of the system's moment arm and mass distribution due to height adjustment, which fundamentally alters the tip-over moment generation mechanism.

## 5. SUMMARY

This paper investigates the anti-tip stability of an adjustable-height single-arm mobile manipulator during warehouse logistics operations. The system architecture and force characteristics of the robot are analyzed, with both the gravity projection method and the tip-over moment (TOM) method employed to model and evaluate stability under static and dynamic conditions. Through co-

simulations using MATLAB and ADAMS, the system's stability was verified under various operating scenarios, including unloaded uniform motion, variable payloads, and different manipulator heights. Results demonstrate that the system maintains satisfactory anti-tip performance under all tested conditions. It should be noted that during loaded operations, both the payload mass and manipulator height significantly affect moment fluctuations, requiring comprehensive control strategies to maintain stability in practical applications. This study establishes a theoretical foundation for subsequent structural parameter optimization and motion control strategies for adjustable-height single-arm mobile manipulators. Based on the stability analysis methodology and system dynamic characteristics developed in this work, future research will focus on formulating effective tip-prevention control strategies to enhance the robot's active safety capabilities in complex working environments.

## ACKNOWLEDGMENTS

This work was supported by the Tianjin Key Research and Development Program Institute City Cooperation Project and Tianjin Municipal Education Commission Research Plan Natural Science Key Project and Tianjin Municipal Education Commission Research Plan Natural Science Key Project [Nos. 23YFYSHZ00280, 2022ZD026, 2022ZD032].

## REFERENCES

- [1] Zhao Yuhang, Chen Cheng, Zhuang Xinghan, et al. Development Review and Prospects of Multi-Mode Mobile Robots[J/OL]. Chinese Journal of Mechanical Engineering, 1-19.
- [2] Wang Liang, Zhou Guofeng, Chen Ya, et al. Traveling Stability Analysis of Logistics Transfer Robot[J]. Journal of Machine Design, 2025, 42(07): 142-149.
- [3] Wu Qilin, Zhao Han, Chen Xiaofei, et al. State of the Art and Development Trends in Multi-Arm Collaborative Robot Technology and Applications[J]. Chinese Journal of Mechanical Engineering, 2023, 59(15): 1-16.
- [4] Zhao Xiangtang, Zhao Yuhang, et al. Stability Analysis of Wheeled Mobile Multi-Robot Coordinated Towing System[J]. Journal of Mechanical Science and Technology, 2022, (prepublish): 1-10.
- [5] Li Yaozhong, Wang Shuting, Jiang Liquan, et al. Motion Planning for Mobile Manipulator Using Sparse Node Rapidly-Exploring Random Tree[J]. China Mechanical Engineering, 2021, 32(12): 1462-1470.
- [6] X. Ding, Y. Liu, J. Hou and Q. Ma, "Online Dynamic Tip-Over Avoidance for a Wheeled Mobile Manipulator With an Improved Tip-Over Moment Stability Criterion," in IEEE Access, vol. 7, pp. 67632-67645, 2019, doi: 10.1109/ACCESS.2019.2915115.
- [7] Song Tao. Research on Tip-Over and Slip Issues of Wheeled Mobile Manipulators[D]. Shanghai University, 2016.
- [8] Zhou Likun, Fu Guiyong. Stability Analysis and Simulation Against Tip-Over for Tank Cleaning Robot[J]. Mechanical Science and Technology for Aerospace Engineering, 2015, 34(04): 533-537.
- [9] Yun Jintian, Deng Lihao, Sang Hongqiang. Motion Stability Analysis of a Wheeled Mobile Humanoid Nursing Robot[J]. China Mechanical Engineering, 2016, 27(17): 2304-2309.
- [10] Zang Jiannan. Structural Design and Performance Analysis of an Articulated Mobile Robot[J]. Science Technology and Engineering, 2022, 22(26): 11465-11471.